

Supporting Information

Bridged Proteolysis Targeting Chimera (PROTAC) Enables Degradation of Undruggable Targets

Yan Xiong^{1#}, Yue Zhong^{1#}, Hyerin Yim^{1#}, Xiaobao Yang¹, Kwang-Su Park¹, Ling Xie², Poulikos I. Poulikakos³, Xiaoran Han⁴, Yue Xiong⁴, Xian Chen², Jing Liu¹, Jian Jin^{1*}

¹ Mount Sinai Center for Therapeutics Discovery, Departments of Pharmacological Sciences, Oncological Sciences and Neuroscience, Tisch Cancer Institute, Icahn School of Medicine at Mount Sinai, New York, New York 10029, USA

² Department of Biochemistry and Biophysics, University of North Carolina at Chapel Hill, Chapel Hill, North Carolina 27599, USA

³ Department of Oncological Sciences, Tisch Cancer Institute, Icahn School of Medicine at Mount Sinai, New York, New York 10029, United States

⁴ Cullgen Inc., San Diego, California 92130, United States

#Y.X., Y.Z., and H.Y. contributed equally to this work.

* Correspondence: jian.jin@mssm.edu

Table of Contents

1. **Figure S1.** Cyclin D1 is frequently amplified in multiple types of human cancer
2. **Figure S2.** The effect of putative PROTACs on degrading cyclin D1
3. **Figure S3.** Quantification of cyclin D1, CDK4 and CDK6 abundance in Calu-1 cells treated with DMSO, MS28, MS28N1, BSJ or PB
4. **Figure S4.** MS28 is more effective in degrading cyclin D1 than CDK4/6 in Calu-1 cells.
5. **Figure S5.** MS28 does not bind cyclin D1, determined using ITC

6. **Figure S6.** MS28 selectively reduces the protein levels of cyclin D1 and cell cycle-related targets in quantitative MS-based proteomic analysis
7. **Figure S7.** Cyclin D1 KO studies in Calu-1 cells
8. **Figure S8.** Quantification of DMSO, MS28, MS28N1, BSJ and PB's effect in Calu-1 cells in the soft agar assay
9. **Figure S9.** Cyclin D1 KO studies in NCI-H2110 cells
10. **Figure S10.** Quantification of cyclin D1, CDK4 and CDK6 abundance in NCI-H2110 cells treated with DMSO, MS28, MS28N1, BSJ or PB
11. **Figure S11.** MS28 effectively degrades cyclin D3 in NCI-H2110 cells
12. **Figure S12.** MS28 preferentially degrades cyclin D1 and cyclin D3 over cyclin D2 and CDK2/4/6 in BT549 cells
13. **Figure S13.** MS28 degrades cyclin D1 and CDK4/6, but is non-toxic, in the PNT2 normal human prostate cell line
14. **Figure S14.** Plasma concentrations of MS28 over 12 h in mice following a single 30 mg/kg intraperitoneal (i.p.) injection
15. **Table S1.** Selectivity of MS28 at 1 μ M against 58 kinases in enzymatic inhibition assays
16. **Table S2.** Proteins significantly downregulated by MS28 in quantitative MS-based proteomic analysis
17. Experimental procedures
18. ^1H NMR spectrum of MS28
19. ^{13}C NMR spectrum of MS28
20. LC-MS spectrum of MS28
21. ^1H NMR spectrum of MS28N1
22. ^{13}C NMR spectrum of MS28N1
23. LC-MS spectrum of MS28N1

24. ^1H NMR spectrum of MS28N2

25. ^{13}C NMR spectrum of MS28N2

26. LC-MS spectrum of MS28N2

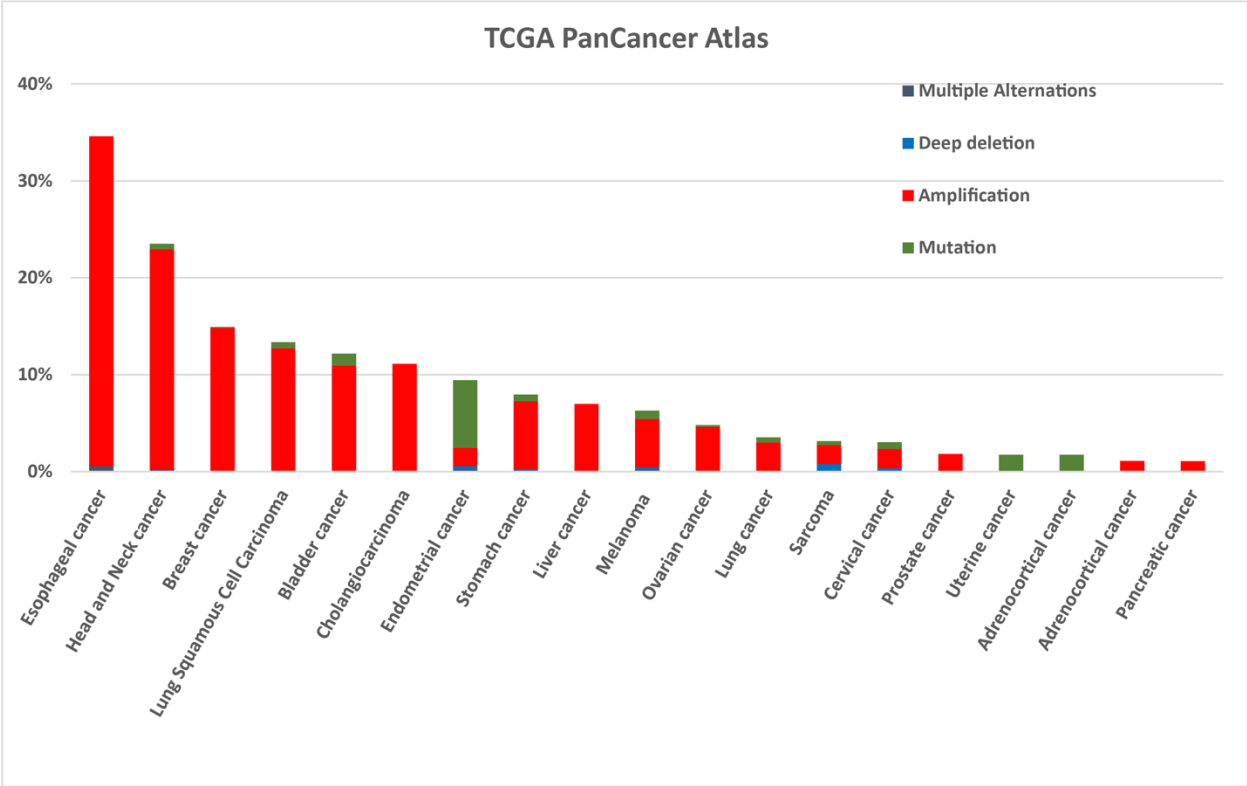


Figure S1. Cyclin D1 is frequently amplified in multiple types of human cancer. Data source: cbioportal.

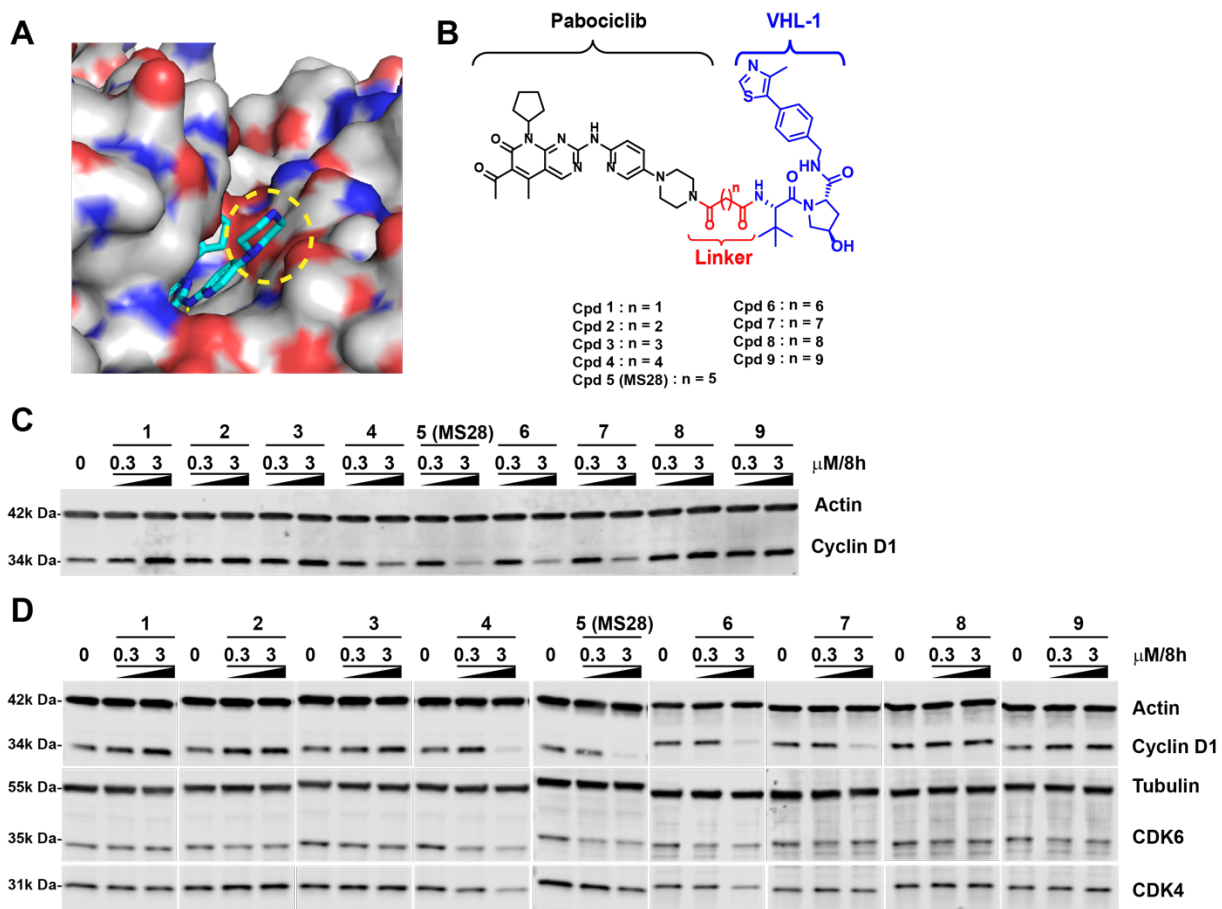


Figure S2. The effect of putative PROTACs on degrading cyclin D1. (A) The cocrystal structure of the CDK6-Palbociclib (PB) complex (PDB ID: 5L2I). The yellow dotted circle highlights the piperazine moiety of PB, which is solvent-exposed. (B) Chemical structures of putative PROTACs designed and synthesized. (C) Western blot (WB) results of compounds 1-9 on degrading cyclin D1 in Calu-1 cells (treated with the indicated compound at the indicated concentration for 8 h). (D) WB results of compounds 1-9 on degrading cyclin D1 and CDK4/6 in Calu-1 cells (treated with the indicated compound at the indicated concentration for 8 h). WB data shown in panels C and D are representative of at least 2 independent experiments.

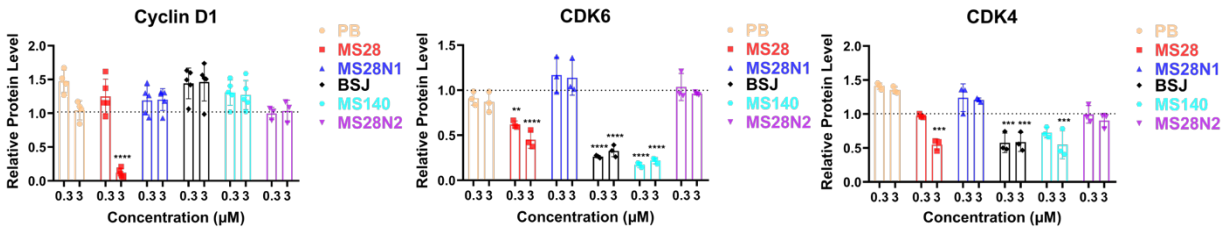


Figure S3. Quantification of cyclin D1, CDK4 and CDK6 abundance in Calu-1 cells treated with DMSO, MS28, MS28N1, BSJ or PB. Calu-1 cells were treated with the indicated compound at the indicated concentrations for 8 h. Protein abundance are calculated relative to DMSO level (protein abundance in DMSO is represented as 1, indicated by the dotted line). P-values are calculated in comparison to DMSO control. ****P < 0.0001. ***P < 0.001. **P < 0.01. Quantifications are calculated based on WB results from at least 2 independent experiments.

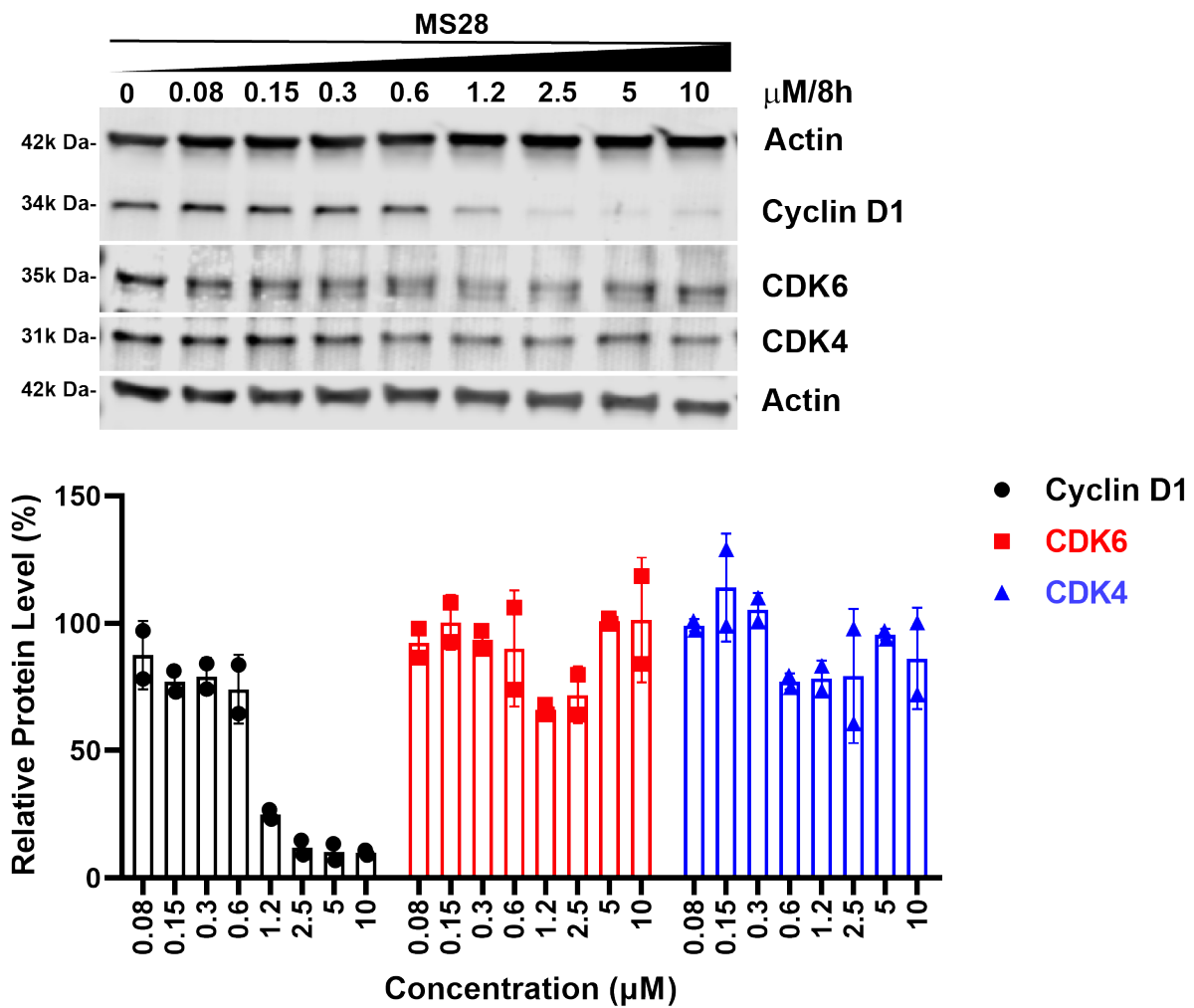


Figure S4. MS28 is more effective in degrading cyclin D1 than CDK4/6 in Calu-1 cells. Up, WB results of cyclin D1 and CDK4/6 in Calu-1 cells treated with MS28 at indicated concentration for 8 h. Down, quantification of cyclin D1, CDK4 and CDK6 abundance in the indicated experimental groups. Protein abundance are calculated relative to DMSO control and data are representative of 2 independent experiments.

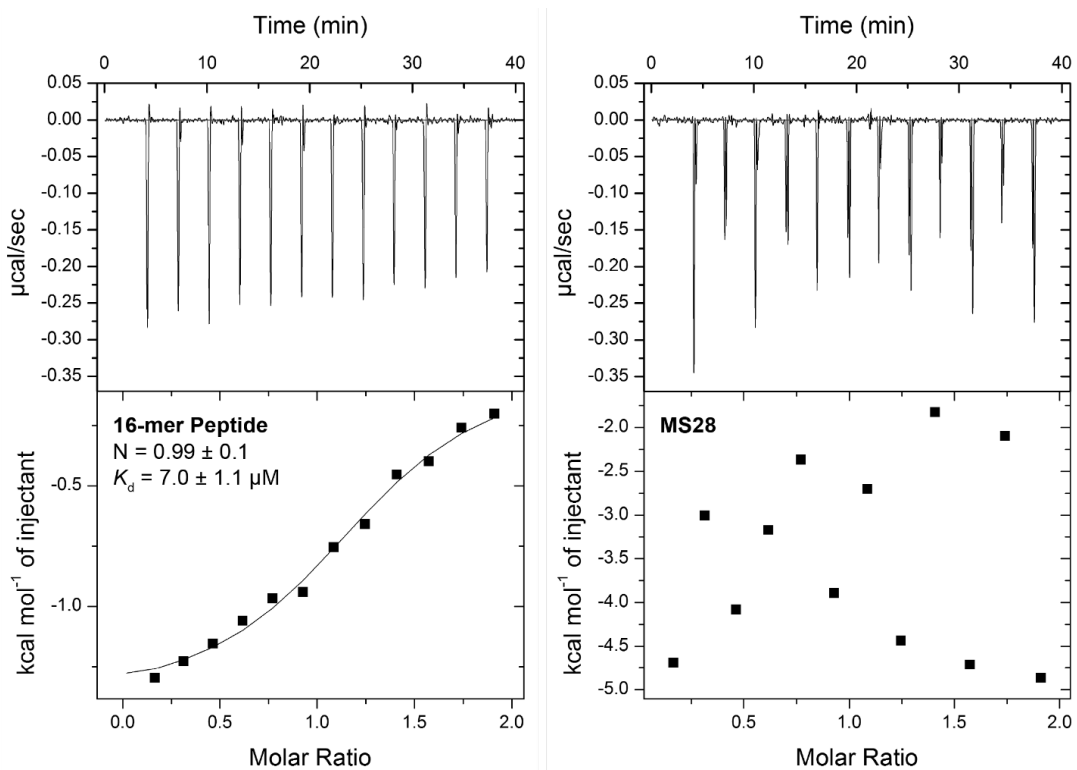


Figure S5. MS28 (right) does not bind cyclin D1 while the positive control (left), a 16-mer peptide (EGVPSTAIRESLLKE) based on the CDK4/6 binding sequence, does. The ITC data are representative of 2 independent experiments. K_d was calculated from the mean of the two independent experiments \pm SD.

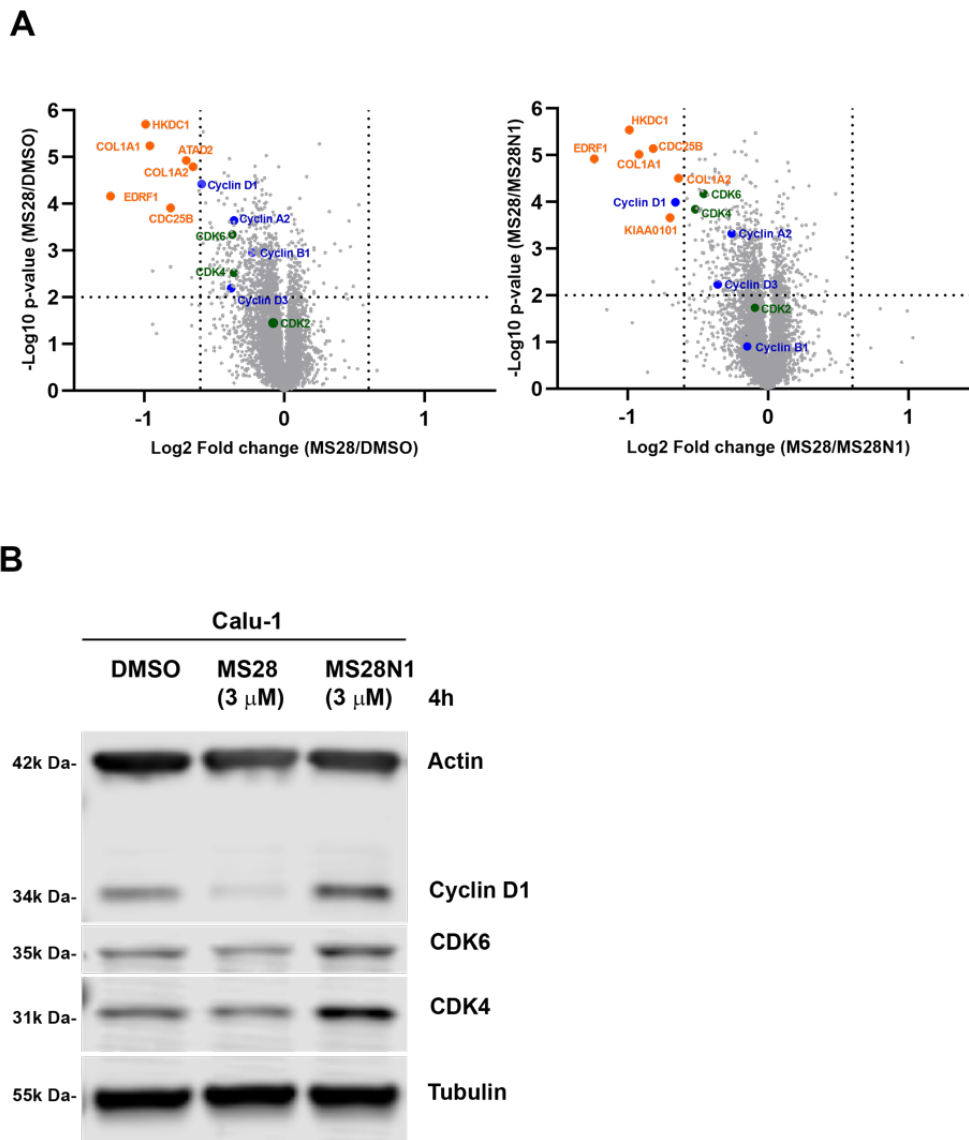


Figure S6. MS28 selectively reduces the protein levels of cyclin D1 and cell-cycle related targets in quantitative MS-based proteomic analysis. (A) Volcano plot of the $-\text{Log}_{10}$ (p value) versus the Log_2 fold change is displayed for MS28 versus DMSO (left) and MS28 versus MS28N1 (right). Calu-1 cells were treated with DMSO or 3 μ M MS28 or MS28N1 for 4 hours. P values were calculated from the data of 3 biological replicates. Dotted lines indicate Log_2 fold change > 0.6 or < -0.6 and $-\text{Log}_{10}$ p value > 2 . (B) The corresponding WB analysis of cyclin D1 and CDK4/6 levels in samples processed for the proteomic study. WB data shown is representative of 3 independent experiments.

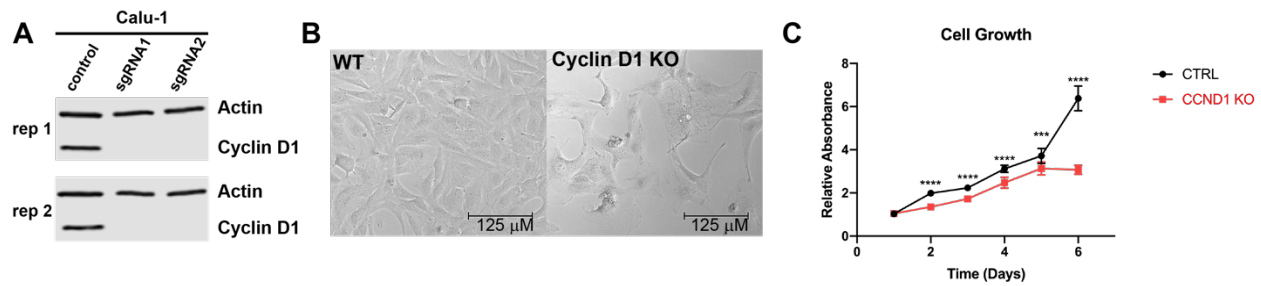


Figure S7. Cyclin D1 KO studies in Calu-1 cells. (A) WB results of two technical repeats confirming CRISPR-mediated *CCND1* KO in Calu-1 cells. (B) CRISPR KO of cyclin D1 significantly suppresses the growth of Calu-1 cells. Growth of WT versus cyclin D1 KO cells were monitored and images from day 6 are displayed. (C) Growth curves of WT versus cyclin D1 KO Calu-1 cells. Results shown are mean \pm SD pooled from 2 independent experiments (each with 5 technical repeats). P-values were calculated by comparing CTRL (control) cell viability to *CCND1* KO cell viability at each day, relative to day 1. ****P < 0.0001; ***P < 0.001.

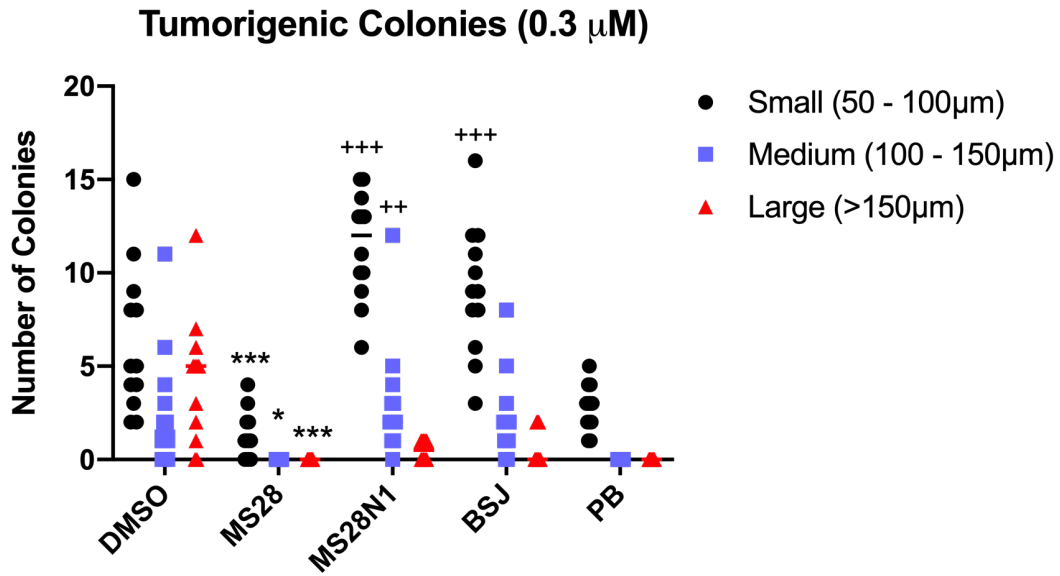


Figure S8. Quantification of DMSO, MS28, MS28N1, BSJ and PB's effect in Calu-1 cells in the soft agar assay. Each point represents one technical repeat. For each technical repeat, 5 images were taken, and the average number of colonies within each size range was calculated. Data were pooled from 3 independent experiments and p-values were calculated in comparison to DMSO (indicated with *) or to MS28 (indicated with +) within each colony size. ***P < 0.001; **P < 0.01; *P < 0.05 (same applies for +).

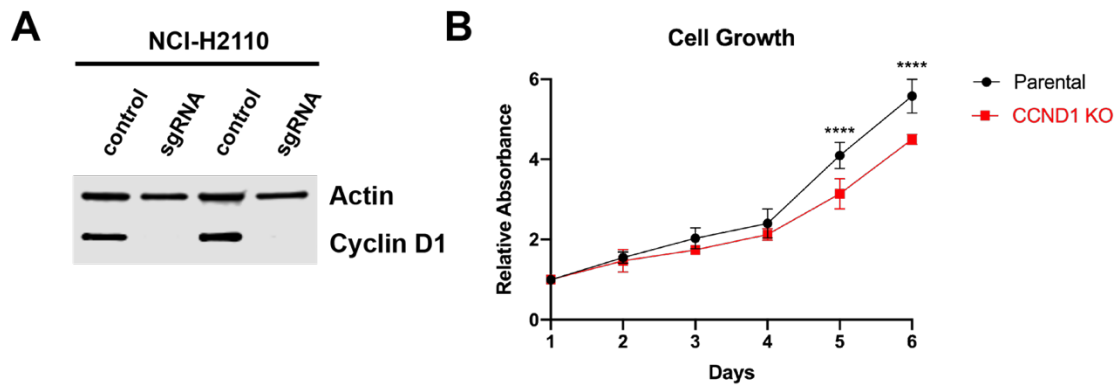


Figure S9. Cyclin D1 KO studies in NCI-H2110 cells. (A) WB results of two technical repeats confirming CRISPR-mediated *CCND1* KO in NCI-H2110 cells. (B) Growth curves of WT versus cyclin D1 KO NCI-H2110 cells. Results shown are mean \pm SD pooled from 2 independent experiments (each with 3 technical repeats). P-values were calculated by comparing parental cell viability to *CCND1* KO cell viability at each day, relative to day 1. ****P < 0.0001.

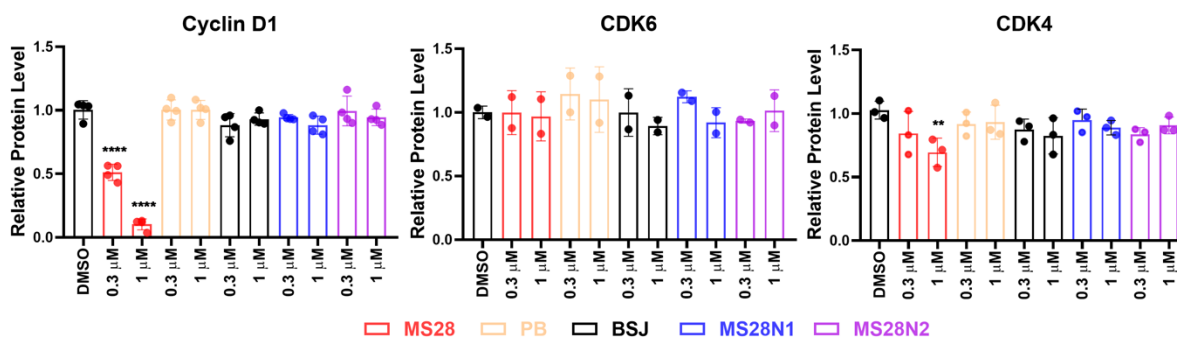


Figure S10. Quantification of cyclin D1, CDK4 and CDK6 abundance in NCI-H2110 cells treated with DMSO, MS28, MS28N1, BSJ or PB. P-values were calculated relative to DMSO control and from 2 independent experiments. ****P < 0.0001. **P < 0.01.

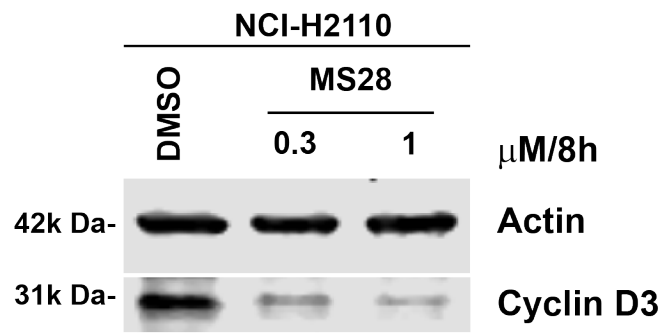


Figure S11. MS28 effectively degrades cyclin D3 in NCI-H2110 cells. NCI-H2110 cells were treated with DMSO or MS28 at the indicated concentrations for 8h. Results are representative of 2 independent experiments.

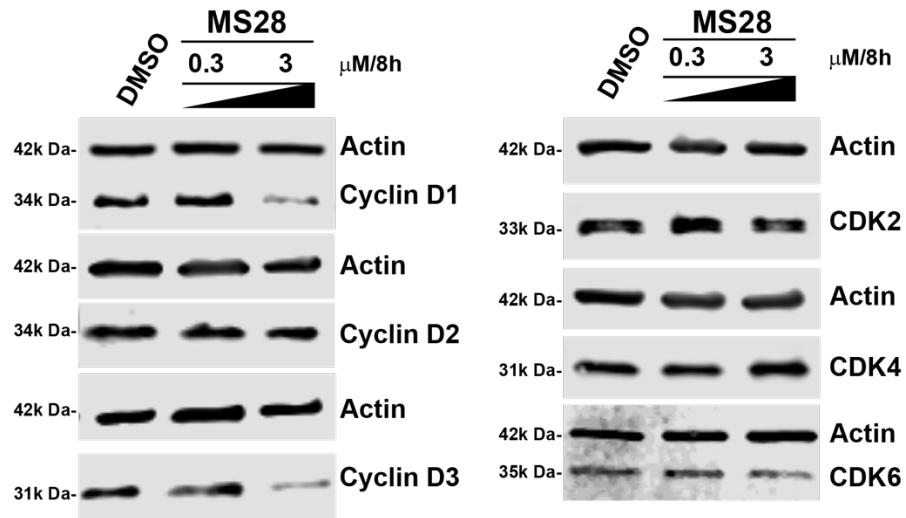


Figure S12. MS28 preferentially degrades cyclin D1 and cyclin D3 over cyclin D2 and CDK2/4/6 in BT549 cells. BT549 cells were treated with DMSO or MS28 at the indicated concentrations for 8 h. Results are representative of 3 independent experiments.

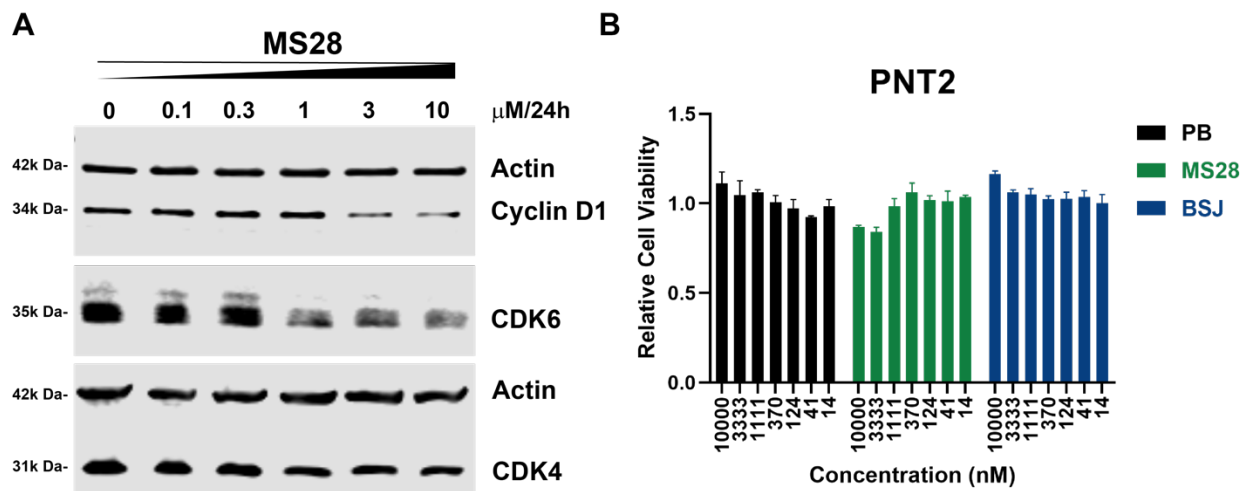


Figure S13. MS28 degrades cyclin D1 and CDK4/6, but is non-toxic, in the PNT2 normal human prostate cell line. (A) WB results display concentration-dependent degradation of cyclin D1 and CDK4/6 in PNT2 cells treated with MS28 for 24 h. WB results shown are representative of 2 independent experiments. (B) PB, MS28 and BSJ are non-toxic in PNT2 cells as they do not significantly inhibit cell growth (treated with indicated compound for 5 days). Data shown are the mean values \pm SD from 2 biological repeats (each with 3 technical repeats).

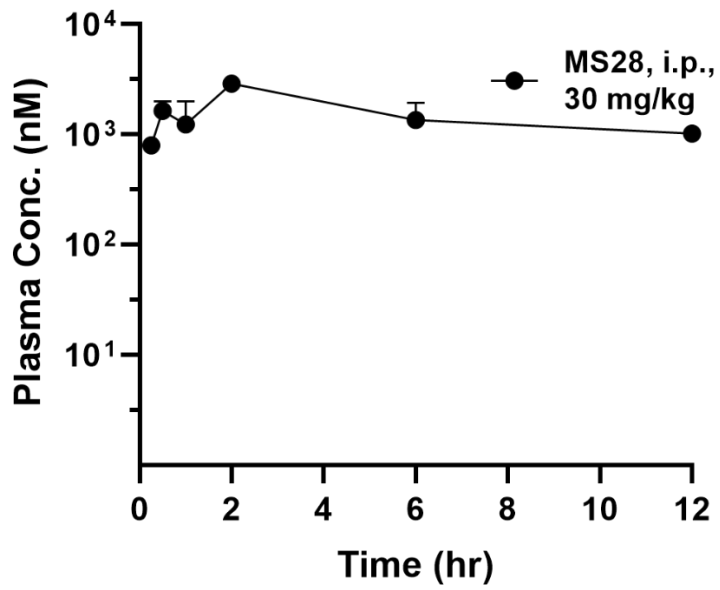


Figure S14. Plasma concentrations of MS28 over 12 h in mice following a single 30 mg/kg intraperitoneal (i.p.) injection. Data represent the mean \pm SD from 3 mice per time point.

Table S1. Selectivity of MS28 at 1 μ M against 58 kinases in enzymatic inhibition assays.

Kinase	Activity (%)	
Abl(h)	100	100
ALK(h)	85	92
AMPK α 1(h)	123	120
ASK1(h)	98	101
Aurora-A(h)	85	86
CaMKI(h)	100	94
CDK1/cyclinB(h)	95	98
CDK2/cyclinA(h)	89	93
CDK6/cyclinD3(h)	9	8
CDK7/cyclinH/MAT1(h)	98	103
CDK9/cyclin T1(h)	56	57
CHK1(h)	92	90
CK1 γ 1(h)	90	87
CK2 α 2(h)	83	82
c-RAF(h)	104	106
DRAK1(h)	90	88
eEF-2K(h)	102	100
EGFR(h)	96	91
EphA5(h)	97	105
EphB4(h)	91	83
Fyn(h)	99	97
GSK3 β (h)	94	96
IGF-1R(h)	104	112
IKK α (h)	107	108
IRAK4(h)	100	97
JAK2(h)	110	110
KDR(h)	110	110
LOK(h)	105	99
Lyn(h)	99	108
MAPKAP-K2(h)	93	98
MEK1(h)	102	100
MLK1(h)	96	101
Mnk2(h)	96	93
MSK2(h)	82	80
MST1(h)	97	92
mTOR(h)	91	96
NEK2(h)	82	87
p70S6K(h)	104	100
PAK2(h)	102	104
PDGFR β (h)	97	101
Pim-1(h)	89	83
PKA(h)	108	102
PKB α (h)	101	99
PKC α (h)	80	78
PKC θ (h)	100	99
PKG1 α (h)	90	98
Plk3(h)	104	102
PRAK(h)	90	100
ROCK-I(h)	100	96
Rse(h)	111	103
Rsk1(h)	77	75
SAPK2a(h)	108	113
SRPK1(h)	107	116

TAK1(h)	97	99
PI3 Kinase (p110 β /p85 α)(h)	94	96
PI3 Kinase (p120 γ)(h)	89	87
PI3 Kinase (p110 δ /p85 α)(h)	51	51
PI3 Kinase (p110 α /p85 α)(h)	76	82

Table S2. Proteins significantly downregulated by MS28 in quantitative MS-based proteomic analysis.

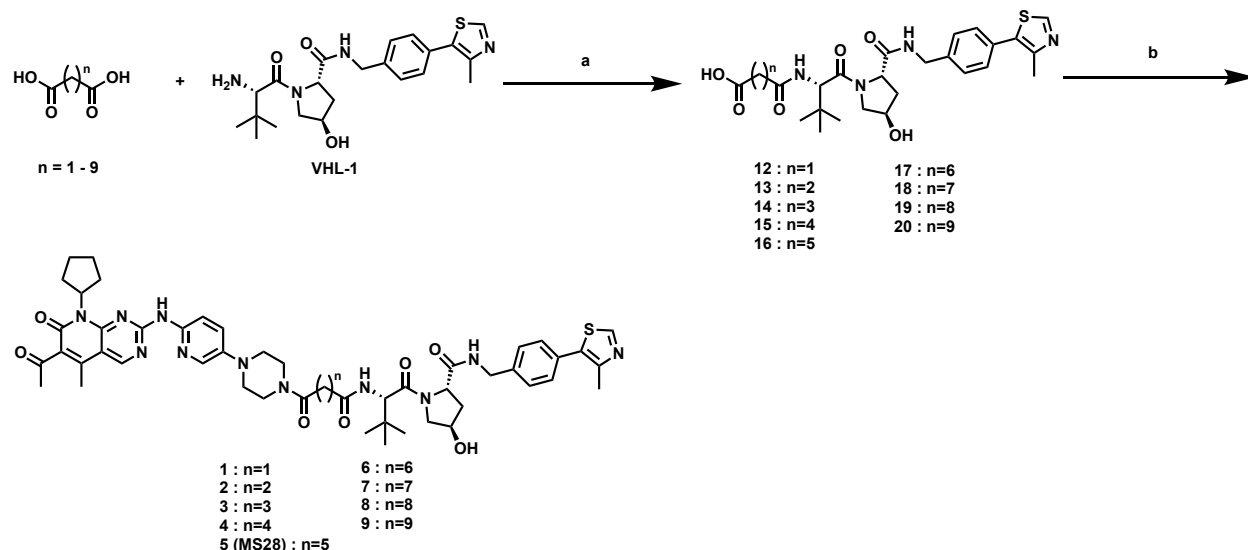
Gene	Function
CCND1	Forms a complex with CDK4/6 to regulate G1/S transition
HKDC1	Hexokinase involved in glucose metabolism ¹
CDC25B	Phosphatase that activates CDC2 (CDK1) by removing inhibitory phosphate groups, thus mediating entry into mitosis.
COL1A1/2	Encodes for the type I collagen
ATAD2	Chromatin regulator that contains an ATPase domain and bromodomain, and is required for DNA replication ² .
EDRF1	May play a role in erythroid cell differentiation.
KIAA0101	Also known as PCLAF (PCNA clamp associated factor); acts as a factor for DNA repair during DNA replication, and plays a role in cell cycle regulation ³ .

Experimental Procedures:

Chemistry

Chemistry General Procedures. All commercial chemical reagents and solvents were used for the reactions without further purification. Microwave-heated reactions were conducted with a Discover SP microwave system with an Explorer 12 Hybrid Autosampler by CEM (Buckingham, UK). Flash column chromatography was performed on Teledyne ISCO CombiFlash RF⁺ instrument equipped with a 220/254/280 nm wavelength UV detector and a fraction collector. Reverse phase column chromatography was conducted on HP C18 RediSep Rf columns to purify some polar compounds. All final compounds were purified with preparative high-performance liquid chromatography (HPLC) on an Agilent Prep 1200 series with the UV detector set to 220/254 nm at a flow rate of 40 mL/min. Samples were injected onto a Phenomenex Luna 750 x 30 mm, 5 μ m C18 column, and the gradient was set to 10% of acetonitrile in H₂O containing 0.1% TFA progressing to 100% of acetonitrile. All compounds assessed for biological activity have purity > 95% as determined by an Agilent 1200 series system with DAD detector and a 2.1 mm x 150 mm Zorbax 300SB-C18 5 μ m column for chromatography and high-resolution mass spectra (HRMS) that were acquired in positive ion mode using an Agilent G1969A API-TOF with an electrospray ionization (ESI) source. Samples (0.5 μ L) were injected onto a C18 column at room temperature, and the flow rate was set to 0.4 mL/min with water containing 0.1% formic acid as solvent A and acetonitrile containing 0.1% formic acid as solvent B. Nuclear magnetic resonance (NMR) spectra were acquired on either Bruker DRX 600 MHz or 400 MHz for proton (¹H NMR) and 151 MHz or 101 MHz for carbon (¹³C NMR). Chemical shifts for all compounds are reported in parts per million (ppm, δ). The format of chemical shift was reported as follows: chemical shift, multiplicity (s = singlet, d = doublet, t = triplet, q = quartet, m = multiplet), coupling constant (*J* values in Hz), and integration. All final compounds had > 95% purity using the HPLC methods described above.

Scheme S1. Synthesis of compound **1-9**^a.



^a Reagents and conditions: (a) TBTU, DIPEA, DMSO, rt, 12 h; (b) PB, TBTU, DIPEA, DMSO, rt, 12 h.

To malonic acid (104 mg, 1.0 mmol) and commercially available VHL-1 (86 mg, 0.20 mmol) in DMSO (3 mL), were added TBTU (70 mg, 0.22 mmol) and DIPEA (0.5 mL, 2.9 mmol) successively. The solution was stirred at room temperature for 12 h followed by purified by reverse-ISCO to yield intermediate **12**, white solid (41 mg, 40% yield). ¹H NMR (400 MHz, Methanol-*d*₄) δ 9.14 (s, 1H), 7.46 – 7.26 (m, 4H), 4.56 (s, 1H), 4.53 – 4.37 (m, 3H), 4.29 (d, $J = 15.6$ Hz, 1H), 3.83 (d, $J = 11.0$ Hz, 1H), 3.71 (d, $J = 10.9$ Hz, 1H), 3.28 – 3.20 (m, 2H), 2.42 (s, 3H), 2.20 – 2.07 (m, 1H), 2.07 – 1.92 (m, 1H), 0.95 (s, 9H).

(2*S*,4*R*)-1-((*S*)-2-(3-(4-(6-((6-acetyl-8-cyclopentyl-5-methyl-7-oxo-7,8-dihydropyrido[2,3-*d*]pyrimidin-2-yl)amino)pyridin-3-yl)piperazin-1-yl)-3-oxopropanamido)-3,3-dimethylbutanoyl)-4-hydroxy-*N*-(4-(4-methylthiazol-5-yl)benzyl)pyrrolidine-2-carboxamide (1**).** To a solution of PB (15 mg, 0.033 mmol) in DMSO (1 mL), intermediate **12** (21 mg, 0.041 mmol), TBTU (14 mg, 0.045 mmol) and DIPEA (0.1 mL, 0.057 mmol) were added

successively. The resulted solution was stirred at room temperature for 12 hours followed by purified by prep-HPLC to yield title compound as yellow solid (9 mg, 30% yield). ¹H NMR (400 MHz, Methanol-*d*₄) δ 9.12 (s, 1H), 8.98 (s, 1H), 8.28 – 8.13 (m, 1H), 7.89 (d, *J* = 2.9 Hz, 1H), 7.56 (d, *J* = 9.6 Hz, 1H), 7.52 – 7.46 (m, 2H), 7.46 – 7.40 (m, 2H), 6.03 (p, *J* = 8.8 Hz, 1H), 4.66 (s, 1H), 4.64 – 4.47 (m, 3H), 4.41 (t, *J* = 14.4 Hz, 1H), 4.05 – 3.53 (m, 6H), 3.44 – 3.25 (m, 6H), 2.52 (s, 3H), 2.50 (s, 3H), 2.45 (s, 3H), 2.39 – 2.28 (m, 2H), 2.27 – 2.18 (m, 1H), 2.18 – 2.04 (m, 3H), 1.92 (s, 2H), 1.79 – 1.65 (m, 2H), 1.09 (s, 9H). HRMS (ESI-TOF) *m/z*: [M+H]⁺ calcd for C₄₉H₆₀N₁₁O₇S, 946.4392; found: 946.4374.

Intermediates **13-20** were prepared following previous reported procedures⁴.

(2*S*,4*R*)-1-((*S*)-2-(4-(4-(6-((6-Acetyl-8-cyclopentyl-5-methyl-7-oxo-7,8-dihydropyrido[2,3-*d*]pyrimidin-2-yl)amino)pyridin-3-yl)piperazin-1-yl)-4-oxobutanamido)-3,3-dimethylbutanoyl)-4-hydroxy-*N*-(4-(4-methylthiazol-5-yl)benzyl)pyrrolidine-2-

carboxamide (2). Compound **2** was synthesized following the same procedure for preparing compound **1** from PB and intermediate **13**. Yellow solid (32 mg, 68% yield). ¹H NMR (600 MHz, Methanol-*d*₄) δ 9.09 (s, 1H), 9.01 (s, 1H), 8.20 (dd, *J* = 9.6, 2.9 Hz, 1H), 7.86 (d, *J* = 2.9 Hz, 1H), 7.53 (d, *J* = 9.6 Hz, 1H), 7.46 (d, *J* = 8.2 Hz, 2H), 7.44 – 7.36 (m, 2H), 6.00 (p, *J* = 8.8 Hz, 1H), 4.61 (s, 1H), 4.58 – 4.47 (m, 3H), 4.36 (d, *J* = 15.5 Hz, 1H), 3.91 – 3.85 (m, 1H), 3.83 – 3.68 (m, 5H), 3.37 – 3.32 (m, 2H), 3.28 – 3.19 (m, 2H), 2.81 – 2.61 (m, 3H), 2.60 – 2.52 (m, 1H), 2.49 (s, 3H), 2.48 (s, 3H), 2.42 (s, 3H), 2.37 – 2.26 (m, 2H), 2.25 – 2.17 (m, 1H), 2.13 – 2.04 (m, 3H), 1.94 – 1.84 (m, 2H), 1.73 – 1.64 (m, 2H), 1.03 (s, 9H). HRMS (ESI-TOF) *m/z*: [M+H]⁺ calcd for C₅₀H₆₂N₁₁O₇S, 960.4549; found: 960.4576.

(2*S*,4*R*)-1-((*S*)-2-(5-(4-(6-((6-Acetyl-8-cyclopentyl-5-methyl-7-oxo-7,8-dihydropyrido[2,3-*d*]pyrimidin-2-yl)amino)pyridin-3-yl)piperazin-1-yl)-5-oxopentanamido)-3,3-dimethylbutanoyl)-4-hydroxy-*N*-(4-(4-methylthiazol-5-yl)benzyl)pyrrolidine-2-

carboxamide (3) Compound **3** was synthesized following the same procedure for preparing compound **1** from PB and intermediate **14**. Yellow solid (40 mg, 77% yield). ¹H NMR (400 MHz, Methanol-*d*₄) δ 9.11 (s, 1H), 8.94 (s, 1H), 8.20 (dd, *J* = 9.8, 2.9 Hz, 1H), 7.88 (d, *J* = 2.8 Hz, 1H), 7.55 (d, *J* = 9.6 Hz, 1H), 7.54 – 7.35 (m, 4H), 6.03 (p, *J* = 8.8 Hz, 1H), 4.64 (s, 1H), 4.63 – 4.45 (m, 3H), 4.39 (d, *J* = 15.5 Hz, 1H), 3.96 (d, *J* = 11.0 Hz, 1H), 3.88 – 3.60 (m, 5H), 3.43 – 3.23 (m, 4H), 2.52 (s, 3H), 2.50 – 2.46 (m, 5H), 2.45 (s, 3H), 2.42 – 2.20 (m, 5H), 2.16 – 2.06 (m, 3H), 2.00 – 1.87 (m, 4H), 1.78 – 1.64 (m, 2H), 1.06 (s, 9H). HRMS (ESI-TOF) *m/z*: [M+H]⁺ calcd for C₅₁H₆₄N₁₁O₇S, 974.4705; found: 974.4706.

(2*S*,4*R*)-1-((*S*)-2-(6-(4-(6-((6-Acetyl-8-cyclopentyl-5-methyl-7-oxo-7,8-dihydropyrido[2,3-*d*]pyrimidin-2-yl)amino)pyridin-3-yl)piperazin-1-yl)-6-oxohexanamido)-3,3-dimethylbutanoyl)-4-hydroxy-*N*-(4-(4-methylthiazol-5-yl)benzyl)pyrrolidine-2-

carboxamide (4) Compound **4** was synthesized following the same procedure for preparing compound **1** from PB and intermediate **15**. Yellow solid (24 mg, 81% yield). ¹H NMR (400 MHz, Methanol-*d*₄) δ 9.01 (s, 1H), 8.89 (s, 1H), 8.12 (dd, *J* = 9.7, 2.9 Hz, 1H), 7.79 (d, *J* = 2.9 Hz, 1H), 7.45 (d, *J* = 9.6 Hz, 1H), 7.43 – 7.28 (m, 4H), 5.93 (p, *J* = 8.8 Hz, 1H), 4.55 (s, 1H), 4.53 – 4.36 (m, 3H), 4.28 (d, *J* = 15.5 Hz, 1H), 3.82 (d, *J* = 11.0 Hz, 1H), 3.78 – 3.61 (m, 5H), 3.32 – 3.10 (m, 4H), 2.42 (s, 3H) 2.39 (s, 3H), 2.35 (s, 3H), 2.30 – 2.19 (m, 4H), 2.18 – 2.09 (m, 1H), 2.07 – 1.94 (m, 3H), 1.89 – 1.75 (m, 2H), 1.68 – 1.53 (m, 6H), 1.30 – 1.27 (m, 2H), 0.96 (s, 9H). HRMS (ESI-TOF) *m/z*: [M+H]⁺ calcd for C₅₂H₆₆N₁₁O₇S, 988.4862; found: 988.4843.

(2*S*,4*R*)-1-((*S*)-2-(7-(4-(6-((6-Acetyl-8-cyclopentyl-5-methyl-7-oxo-7,8-dihydropyrido[2,3-*d*]pyrimidin-2-yl)amino)pyridin-3-yl)piperazin-1-yl)-7-oxoheptanamido)-3,3-dimethylbutanoyl)-4-hydroxy-*N*-(4-(4-methylthiazol-5-yl)benzyl)pyrrolidine-2-

carboxamide (MS28, 5) MS28 was synthesized following the same procedure for preparing compound **1** from PB and intermediate **16**. Yellow solid (20 mg, 68% yield). ¹H NMR (400 MHz, DMSO-*d*₆) δ 10.25 (s, 1H), 8.90 (s, 2H), 8.52 (t, *J* = 6.1 Hz, 1H), 8.02 (s, 1H), 7.90 – 7.73 (m, 2H), 7.44 – 7.22 (m, 5H), 5.86 – 5.64 (m, 1H), 5.12 (s, 1H), 4.52 (d, *J* = 9.2 Hz, 1H), 4.46 – 4.36 (m, 2H), 4.33 (s, 1H), 4.18 (dd, *J* = 16.0, 5.3 Hz, 1H), 3.73 – 3.49 (m, 6H), 3.19 – 2.96 (m, 4H), 2.39 (s, 3H), 2.37 (s, 3H), 2.32 – 2.15 (m, 7H), 2.03 (s, 3H), 1.94 – 1.79 (m, 3H), 1.79 – 1.66 (m, 2H), 1.63 – 1.39 (m, 6H), 1.32 – 1.18 (m, 2H), 0.90 (s, 9H). ¹³C NMR (101 MHz, DMSO-*d*₆) δ 200.71, 170.50, 170.34, 169.05, 168.12, 159.10, 156.64, 156.44, 153.10, 149.70, 146.05, 143.10, 141.39, 140.48, 137.83, 134.26, 129.53, 128.00, 127.60, 126.97, 125.78, 116.39, 112.87, 104.87, 77.53, 67.29, 57.10, 54.75, 54.71, 51.43, 47.28, 46.86, 43.02, 40.05, 39.06, 36.31, 33.57, 33.20, 30.52, 29.63, 26.84, 25.91, 24.75, 23.69, 23.51, 22.94, 14.28, 11.95, -0.50. HRMS (ESI-TOF) *m/z*: [M+H]⁺ calcd for C₅₃H₆₈N₁₁O₇S, 1002.5018; found: 1002.5029.

(2*S*,4*R*)-1-((*S*)-2-(8-(4-(6-((6-Acetyl-8-cyclopentyl-5-methyl-7-oxo-7,8-dihydropyrido[2,3-*d*]pyrimidin-2-yl)amino)pyridin-3-yl)piperazin-1-yl)-8-oxooctanamido)-3,3-dimethylbutanoyl)-4-hydroxy-*N*-(4-(4-methylthiazol-5-yl)benzyl)pyrrolidine-2-

carboxamide (6) Compound **6** was synthesized following the same procedure for preparing compound **1** from PB and intermediate **17**. Yellow solid (68 mg, 60% yield). ¹H NMR (400 MHz, Methanol-*d*₄) δ 9.12 (s, 1H), 8.98 (s, 1H), 8.22 (dd, *J* = 9.7, 2.9 Hz, 1H), 7.88 (d, *J* = 2.9 Hz, 1H), 7.56 (d, *J* = 9.6 Hz, 1H), 7.52 – 7.39 (m, 4H), 6.03 (p, *J* = 8.8 Hz, 1H), 4.66 (s, 1H), 4.64 – 4.46 (m, 3H), 4.38 (d, *J* = 15.5 Hz, 1H), 3.93 (d, *J* = 11.0 Hz, 1H), 3.87 – 3.71 (m, 5H), 3.43 – 3.21 (m, 4H), 2.52 – 2.45 (m, 11H), 2.39 – 2.20 (m, 5H), 2.17 – 2.04 (m, 3H), 1.98 – 1.86 (m, 2H), 1.78 –

1.59 (m, 6H), 1.47 – 1.34 (m, 4H), 1.05 (s, 9H). HRMS (ESI-TOF) m/z : $[M+H]^+$ calcd for $C_{54}H_{70}N_{11}O_7S$, 1016.5175; found: 1016.5177.

(2*S*,4*R*)-1-((*S*)-2-(9-(4-(6-((6-acetyl-8-cyclopentyl-5-methyl-7-oxo-7,8-dihydropyrido[2,3-*d*]pyrimidin-2-yl)amino)pyridin-3-yl)piperazin-1-yl)-9-oxononanamido)-3,3-dimethylbutanoyl)-4-hydroxy-*N*-(4-(4-methylthiazol-5-yl)benzyl)pyrrolidine-2-

carboxamide (7) Compound **7** was synthesized following the same procedure for preparing compound **1** from PB and intermediate **18**. Yellow solid (17 mg, 67% yield). 1H NMR (600 MHz, Methanol- d_4) δ 9.10 (s, 1H), 9.00 (s, 1H), 8.20 (dd, $J = 9.6, 3.0$ Hz, 1H), 7.86 (d, $J = 3.0$ Hz, 1H), 7.54 (d, $J = 9.6$ Hz, 1H), 7.46 (d, $J = 8.0$ Hz, 2H), 7.41 (d, $J = 8.1$ Hz, 2H), 6.00 (p, $J = 8.9$ Hz, 1H), 4.63 (s, 1H), 4.60 – 4.45 (m, 3H), 4.36 (d, $J = 15.5$ Hz, 1H), 3.90 (d, $J = 11.0$ Hz, 1H), 3.82 – 3.74 (m, 5H), 3.35 – 3.32 (m, 2H), 3.26 (t, $J = 5.4$ Hz, 2H), 2.51 – 2.44 (m, 8H), 2.43 (s, 3H), 2.32 – 2.19 (m, 5H), 2.13 – 2.04 (m, 3H), 1.95 – 1.85 (m, 2H), 1.74 – 1.66 (m, 2H), 1.65 – 1.57 (m, 4H), 1.39 – 1.32 (m, 6H), 1.03 (s, 9H). HRMS (ESI-TOF) m/z : $[M+H]^+$ calcd for $C_{55}H_{72}N_{11}O_7S$, 1030.5331; found: 1030.5345.

(2*S*,4*R*)-1-((*S*)-2-(10-(4-(6-((6-acetyl-8-cyclopentyl-5-methyl-7-oxo-7,8-dihydropyrido[2,3-*d*]pyrimidin-2-yl)amino)pyridin-3-yl)piperazin-1-yl)-10-oxodecanamido)-3,3-dimethylbutanoyl)-4-hydroxy-*N*-(4-(4-methylthiazol-5-yl)benzyl)pyrrolidine-2-

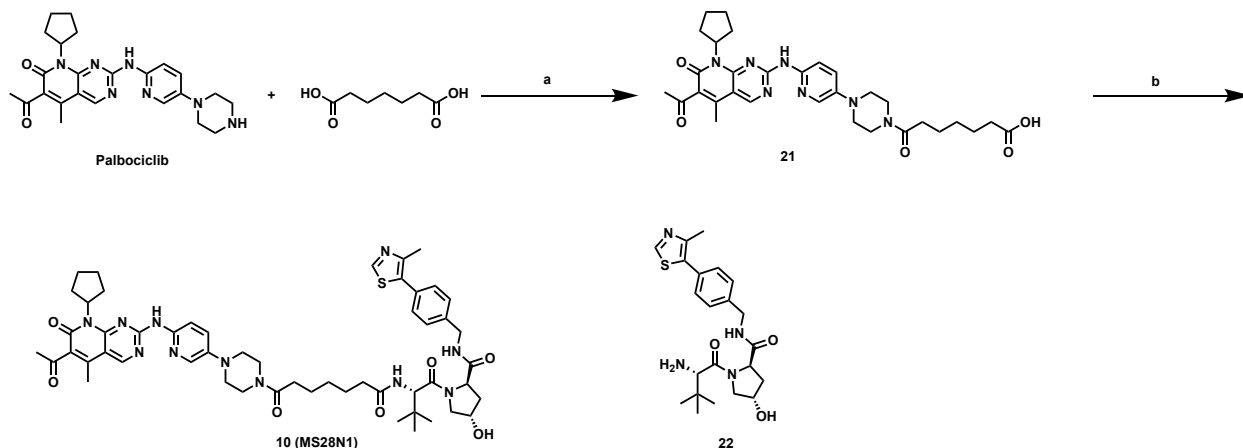
carboxamide (8) Compound **8** was synthesized following the same procedure for preparing compound **1** from PB and intermediate **19**. Yellow solid (25 mg, 54%) 1H NMR (600 MHz, Methanol- d_4) δ 9.09 (s, 1H), 8.93 (s, 1H), 8.19 (dd, $J = 9.6, 3.0$ Hz, 1H), 7.87 (d, $J = 3.0$ Hz, 1H), 7.54 (d, $J = 9.6$ Hz, 1H), 7.46 (d, $J = 8.2$ Hz, 2H), 7.41 (d, $J = 8.3$ Hz, 2H), 6.00 (p, $J = 8.9$ Hz, 1H), 4.63 (s, 1H), 4.61 – 4.45 (m, 3H), 4.35 (d, $J = 15.5$ Hz, 1H), 3.96 – 3.86 (m, 1H), 3.82 – 3.74 (m, 5H), 3.33 – 3.31 (m, 2H), 3.27 (t, $J = 5.3$ Hz, 2H), 2.49 (s, 3H), 2.48 – 2.41 (m, 8H), 2.34 –

2.18 (m, 5H), 2.12 – 2.04 (m, 3H), 1.94 – 1.85 (m, 2H), 1.74 – 1.66 (m, 2H), 1.66 – 1.55 (m, 4H), 1.41 – 1.30 (m, 8H), 1.03 (s, 9H). HRMS (ESI-TOF) m/z : $[M+H]^+$ calcd for $C_{56}H_{74}N_{11}O_7S$, 1044.5448; found: 1044.5468.

(2*S*,4*R*)-1-((*S*)-2-(11-(4-(6-((6-Acetyl-8-cyclopentyl-5-methyl-7-oxo-7,8-dihydropyrido[2,3-*d*]pyrimidin-2-yl)amino)pyridin-3-yl)piperazin-1-yl)-11-oxoundecanamido)-3,3-dimethylbutanoyl)-4-hydroxy-*N*-(4-(4-methylthiazol-5-yl)benzyl)pyrrolidine-2-

carboxamide (9) Compound **9** was synthesized following the same procedure for preparing compound **1** from PB and intermediate **20**. Yellow solid (17 mg, 67% yield). 1H NMR (600 MHz, Methanol- d_4) δ 9.10 (s, 1H), 8.94 (s, 1H), 8.20 (dd, $J = 9.6, 2.9$ Hz, 1H), 7.86 (d, $J = 3.0$ Hz, 1H), 7.54 (d, $J = 9.5$ Hz, 1H), 7.46 (d, $J = 8.1$ Hz, 2H), 7.41 (d, $J = 8.2$ Hz, 2H), 6.01 (p, $J = 8.8$ Hz, 1H), 4.63 (s, 1H), 4.60 – 4.44 (m, 3H), 4.35 (d, $J = 15.5$ Hz, 1H), 3.90 (d, $J = 11.0$ Hz, 1H), 3.85 – 3.71 (m, 5H), 3.35 – 3.22 (m, 4H), 2.50 (s, 3H), 2.49 – 2.41 (m, 8H), 2.35 – 2.27 (m, 3H), 2.27 – 2.18 (m, 2H), 2.13 – 2.04 (m, 3H), 1.94 – 1.85 (m, 2H), 1.73 – 1.66 (m, 2H), 1.66 – 1.56 (m, 4H), 1.38 – 1.29 (m, 10H), 1.03 (s, 9H). HRMS (ESI-TOF) m/z : $[M+H]^+$ calcd for $C_{57}H_{76}N_{11}O_7S$, 1058.5644; found: 1058.5631.

Scheme S2. Synthesis of MS28N1 (compound **10**)^a.



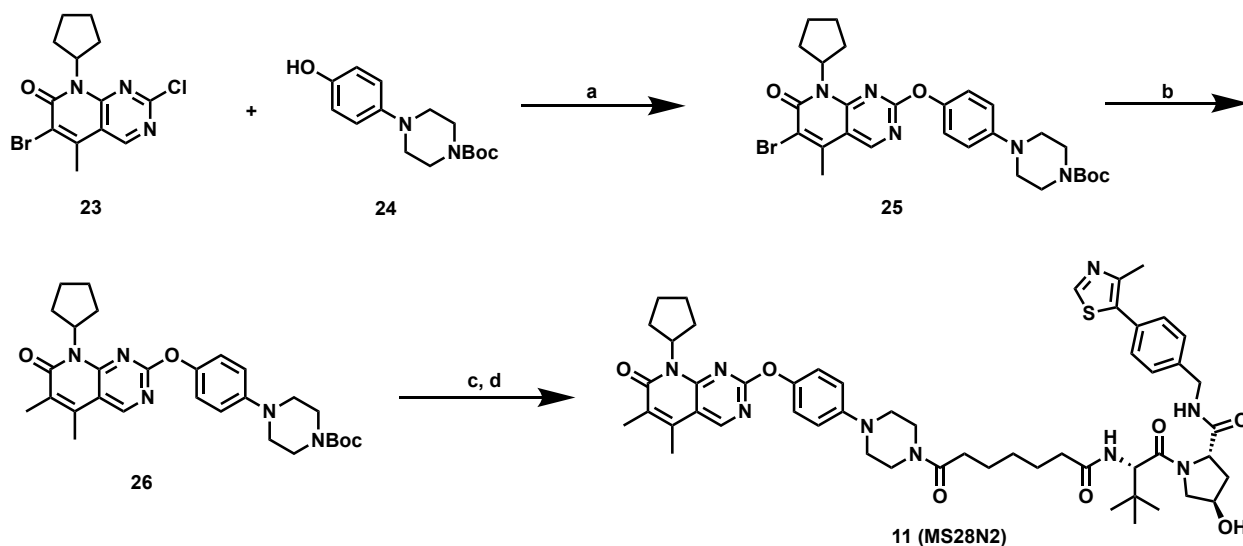
^a Reagents and conditions: (a) TBTU, DIPEA, DMSO, rt, 12 h; (b) **22**, TBTU, DIPEA, DMSO, rt, 12 h.

To a solution of PB (45 mg, 0.10 mmol) in DMSO (3 mL), heptanedioic acid (157 mg, 0.98 mmol), TBTU (38 mg, 0.12 mmol) and DIPEA (0.1 mL, 0.57 mmol) were added successively. The solution was stirred at room temperature for 12 hour followed by purified by prep-HPLC to yield intermediate **21**, yellow solid (60 mg, 85% yield). ¹H NMR (600 MHz, Methanol-*d*₄) δ 9.12 (s, 1H), 8.23 (dd, *J* = 9.7, 2.9 Hz, 1H), 7.90 (d, *J* = 3.0 Hz, 1H), 7.57 (d, *J* = 9.6 Hz, 1H), 6.03 (p, *J* = 8.9 Hz, 1H), 3.89 – 3.71 (m, 4H), 3.36 (t, *J* = 5.2 Hz, 2H), 3.31 (t, *J* = 5.3 Hz, 2H), 2.53 – 2.48 (m, 5H), 2.45 (s, 3H), 2.37 – 2.30 (m, 4H), 2.16 – 2.07 (m, 2H), 1.98 – 1.88 (m, 2H), 1.76 – 1.61 (m, 6H), 1.49 – 1.41 (m, 2H).

(2*R*,4*S*)-1-((*S*)-2-(7-(4-(6-((6-acetyl-8-cyclopentyl-5-methyl-7-oxo-7,8-dihydropyrido[2,3-*d*]pyrimidin-2-yl)amino)pyridin-3-yl)piperazin-1-yl)-7-oxoheptanamido)-3,3-dimethylbutanoyl)-4-hydroxy-*N*-(4-(4-methylthiazol-5-yl)benzyl)pyrrolidine-2-carboxamide (MS28N1, **10)**. To a solution of intermediate **21** (60 mg, 0.085 mmol) in DMSO (2 mL), commercially available intermediate **22** (60 mg, 0.14 mmol) and TBTU (51 mg, 0.16 mmol) and DIPEA (0.1 mL, 0.057 mmol) were added successively. The solution was stirred at room

temperature for 12 hour followed by purified by prep-HPLC to yield title compound. Yellow solid (62 mg, 65% yield). ^1H NMR (400 MHz, Methanol- d_4) δ 9.10 (s, 2H), 8.19 (dd, $J = 9.7, 3.0$ Hz, 1H), 7.86 (d, $J = 2.9$ Hz, 1H), 7.54 (d, $J = 9.6$ Hz, 1H), 7.46 (d, $J = 8.3$ Hz, 2H), 7.41 (d, $J = 8.3$ Hz, 2H), 6.00 (p, $J = 8.8$ Hz, 1H), 4.58 (dd, $J = 8.4, 6.5$ Hz, 1H), 4.54 – 4.43 (m, 3H), 4.38 (d, $J = 15.6$ Hz, 1H), 4.00 (dd, $J = 10.9, 4.9$ Hz, 1H), 3.83 – 3.66 (m, 5H), 3.30 – 3.23 (m, 4H), 2.51 (s, 3H), 2.50 (s, 3H), 2.43 (s, 3H), 2.39 (t, $J = 7.6$ Hz, 2H), 2.35 – 2.05 (m, 8H), 1.97 – 1.84 (m, 2H), 1.77 – 1.63 (m, 2H), 1.61 – 1.42 (m, 4H), 1.35 – 1.27 (m, 2H), 1.08 (s, 9H). ^{13}C NMR (101 MHz, DMSO- d_6) δ 202.94, 173.54, 172.11, 171.11, 170.28, 161.21, 158.94, 158.69, 155.21, 151.88, 148.21, 145.24, 143.63, 142.55, 139.80, 136.39, 131.60, 130.19, 129.75, 129.24, 127.80, 125.80, 115.43, 107.08, 79.63, 68.94, 59.29, 57.59, 55.73, 53.41, 49.38, 48.97, 45.08, 42.04, 41.13, 38.35, 35.06, 34.69, 32.55, 31.77, 28.84, 28.03, 26.96, 26.92, 25.63, 25.62, 25.01, 16.44, 14.09. HRMS (ESI-TOF) m/z : $[\text{M}+\text{H}]^+$ calcd for $\text{C}_{53}\text{H}_{68}\text{N}_{11}\text{O}_7\text{S}$, 1002.5018; found: 1002.5027.

Scheme S3. Synthesis of MS28N2 (compound **11**)^a.



^aReagents and conditions: (a) Cs₂CO₃, THF, MW, 100°C, 30 min; (b) Trimethylboroxine, XPhos-Pd-G2, K₃PO₄, dioxane/H₂O, MW, 130°C, 30 min; (c) 4N HCl in dioxane, rt, 1 h; (d) **16**, TBTU, DIEA, DMSO, rt, 1 h.

Commercially available intermediates **23** (120 mg, 0.35 mmol) and **24** (125 mg, 0.45 mmol) were mixed together in a 10 mL microwave reaction tube, following by Cs₂CO₃ (293 mg, 0.9 mmol) and THF (3 mL). The mixture was heated under microwave irradiation condition at 100°C for 30 min. After cooling down, the mixture was filtered and the filtrate was collected. The solvent was removed, the residue was purified by flash silica gel column to yield intermediate **25** (202 mg, 99%) as white solid. ¹H NMR (600 MHz, Chloroform-*d*) δ 8.84 (s, 1H), 7.08 (d, *J* = 9.0 Hz, 2H), 6.96 (d, *J* = 9.0 Hz, 2H), 5.77 (p, *J* = 8.9 Hz, 1H), 3.61 – 3.57 (m, 4H), 3.55 (t, *J* = 5.1 Hz, 1H), 3.12 (t, *J* = 5.1 Hz, 4H), 2.96 (t, *J* = 5.1 Hz, 1H), 2.61 (s, 3H), 2.18 – 2.07 (m, 2H), 1.80 – 1.71 (m, 2H), 1.71 – 1.58 (m, 2H), 1.48 (s, 9H).

Intermediate **25** (63 mg, 0.11 mmol), trimethylboroxine (32 mg, 0.25 mmol), Xphos-Pd-G2 (23 mg, 0.026 mmol), K₃PO₄ (66 mg, 0.31 mmol), dioxane/H₂O (10:1, 2.2 mL) were added into a 10 mL microwave reaction tube successively. The mixture was heated under microwave irradiation condition at 130°C for 30 min. After cooling down, the mixture was filtered and the filtrate was collected. The solvent was removed, the residue was purified by prep-HPLC to yield intermediate **26** (22 mg, 38%) as brown oil. ¹H NMR (400 MHz, Methanol-*d*₄) δ 8.95 (s, 1H), 7.17 (d, *J* = 8.1 Hz, 4H), 5.61 (q, *J* = 9.0, 8.2 Hz, 1H), 3.69 – 3.60 (m, 4H), 3.27 – 3.18 (m, 4H), 2.48 (s, 3H), 2.17 (s, 3H), 2.15 – 2.05 (m, 2H), 1.70 – 1.57 (m, 2H), 1.48 (s, 9H), 1.47 – 1.34 (m, 4H).

(2*S*,4*R*)-1-((*S*)-2-(7-(4-(4-((8-cyclopentyl-5,6-dimethyl-7-oxo-7,8-dihydropyrido[2,3-*d*]pyrimidin-2-yl)oxy)phenyl)piperazin-1-yl)-7-oxoheptanamido)-3,3-dimethylbutanoyl)-4-hydroxy-*N*-(4-(4-methylthiazol-5-yl)benzyl)pyrrolidine-2-carboxamide (MS28N2, **11**)

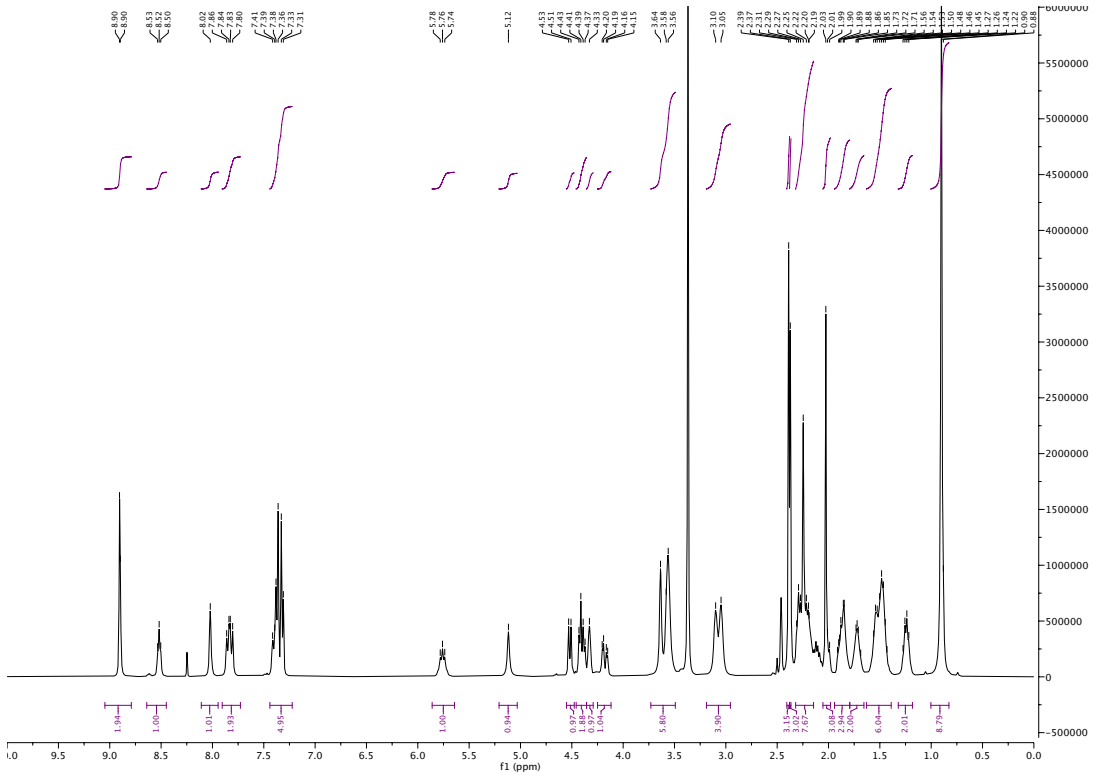
Intermediate **26** (22 mg, 0.042 mmol) was mixed with HCl dioxane solution (4N, 0.5 mL, 2 mmol),

the mixture was stirred at room temperature for 2 h, following by concentrated. The resulted white solid reacted with intermediate **16** following the same procedure for MS28 to yield compound **11**, white solid (26 mg, 57% yield in 2 steps). ¹H NMR (400 MHz, Methanol-*d*₄) δ 8.95 (s, 2H), 7.48 (d, *J* = 8.1 Hz, 2H), 7.41 (d, *J* = 7.2 Hz, 2H), 7.15 – 7.06 (m, 4H), 5.62 (p, *J* = 9.2 Hz, 1H), 4.66 (s, 1H), 4.63 – 4.49 (m, 3H), 4.37 (d, *J* = 15.5 Hz, 1H), 3.93 (d, *J* = 11.0 Hz, 1H), 3.87 – 3.68 (m, 5H), 3.28 – 3.10 (m, 4H), 2.53 – 2.40 (m, 8H), 2.39 – 2.19 (m, 3H), 2.17 (s, 3H), 2.15 – 2.05 (m, 3H), 1.75 – 1.54 (m, 6H), 1.53 – 1.32 (m, 6H), 1.05 (s, 9H). ¹³C NMR (101 MHz, Methanol-*d*₄) δ 174.47, 173.08, 172.65, 170.93, 163.98, 163.42, 156.82, 154.99, 151.65, 148.86, 147.21, 146.89, 139.76, 139.03, 132.25, 129.88, 128.94, 127.62, 126.31, 121.97, 117.87, 110.79, 69.69, 59.44, 57.59, 56.65, 54.04, 50.34, 49.86, 45.42, 42.30, 41.35, 37.56, 35.16, 35.04, 32.41, 28.51, 27.19, 25.68, 25.32, 24.80, 24.32, 14.31, 12.81, 12.02. HRMS (ESI-TOF) *m/z*: [M+H]⁺ calcd for C₅₃H₆₈N₉O₇S, 974.4957; found: 974.49.

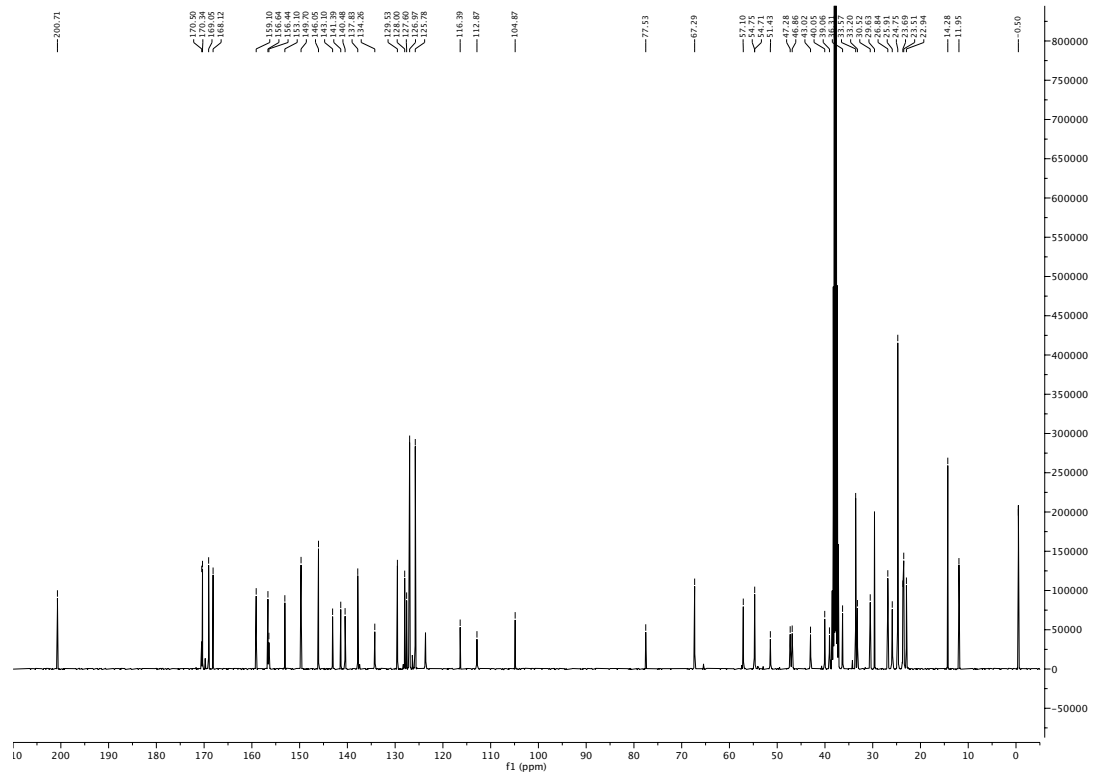
References

1. Ludvik, A. E.; Pusec, C. M.; Priyadarshini, M.; Angueira, A. R.; Guo, C.; Lo, A.; Hershenhouse, K. S.; Yang, G.-Y.; Ding, X.; Reddy, T. E.; Lowe, W. L., Jr; Layden, B. T., HKDC1 is a novel hexokinase involved in whole-body glucose use. *Endocrinology* **2016**, *157* (9), 3452-3461.
2. Chacin, E.; Bansal, P.; Reuswig, K.-U.; Diaz-Santin, L. M.; Ortega, P.; Vizjak, P.; Gómez-González, B.; Müller-Planitz, F.; Aguilera, A.; Pfander, B.; Cheung, A. C. M.; Kurat, C. F., A CDK-regulated chromatin segregase promoting chromosome replication. *Nat. Comm.* **2021**, *12* (1), 5224.
3. Emanuele, M. J.; Ciccia, A.; Elia, A. E.; Elledge, S. J., Proliferating cell nuclear antigen (PCNA)-associated KIAA0101/PAF15 protein is a cell cycle-regulated anaphase-promoting complex/cyclosome substrate. *Proc. Natl. Acad. Sci. U. S. A.* **2011**, *108* (24), 9845-9850.

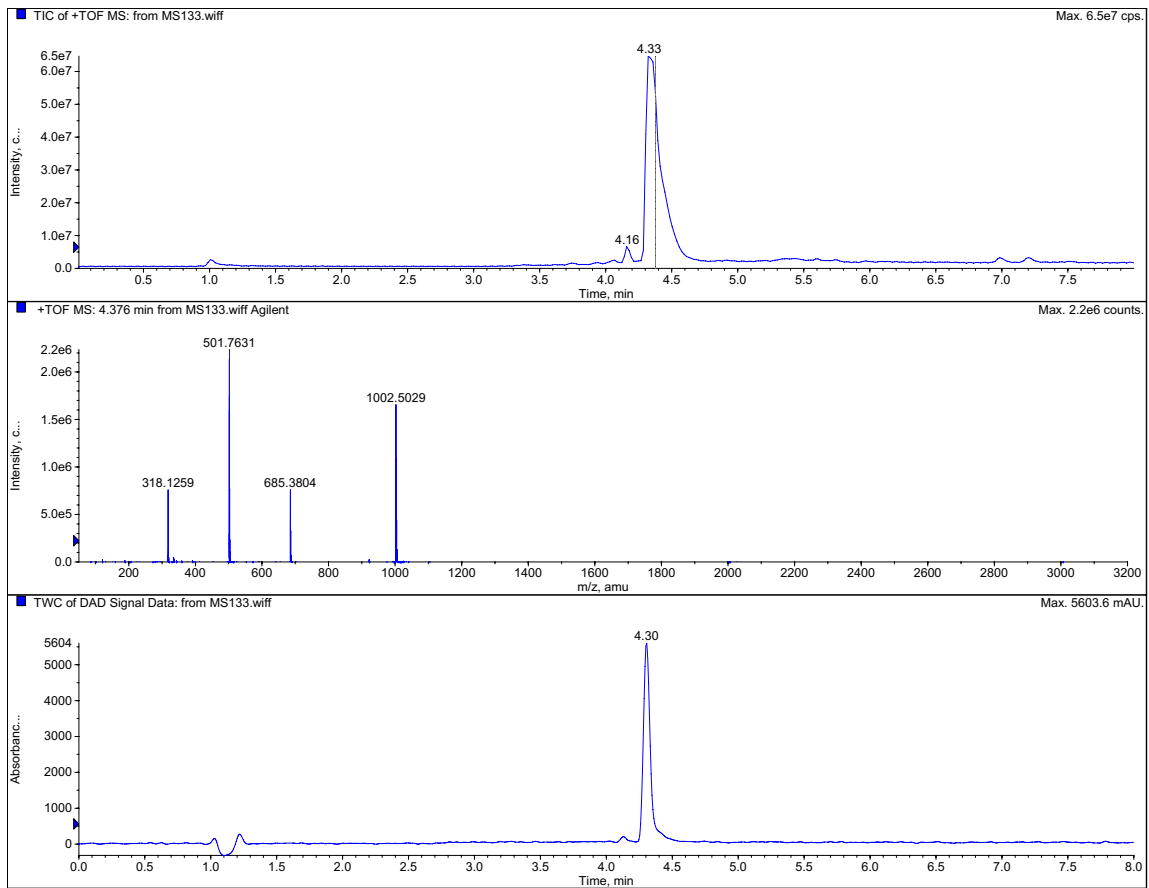
4. Jin, J. Y., X.; Liu, J.; Xiong, Y.; Poulikakos, P.; Karoulia, Z.; Wu, X.; Ahmed, T.,
Compositions and methods for treating CDK4/6-mediated cancer. *International Patent
Application* **2018**, *WO 2018106870*.



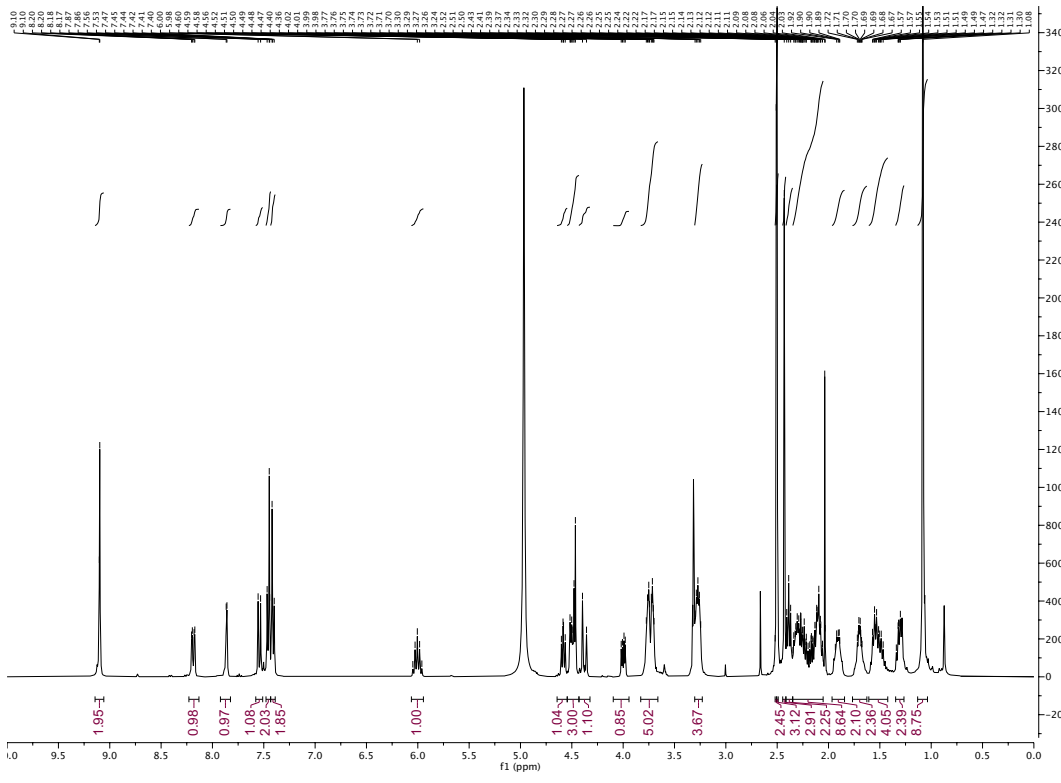
¹H NMR spectrum of MS28.



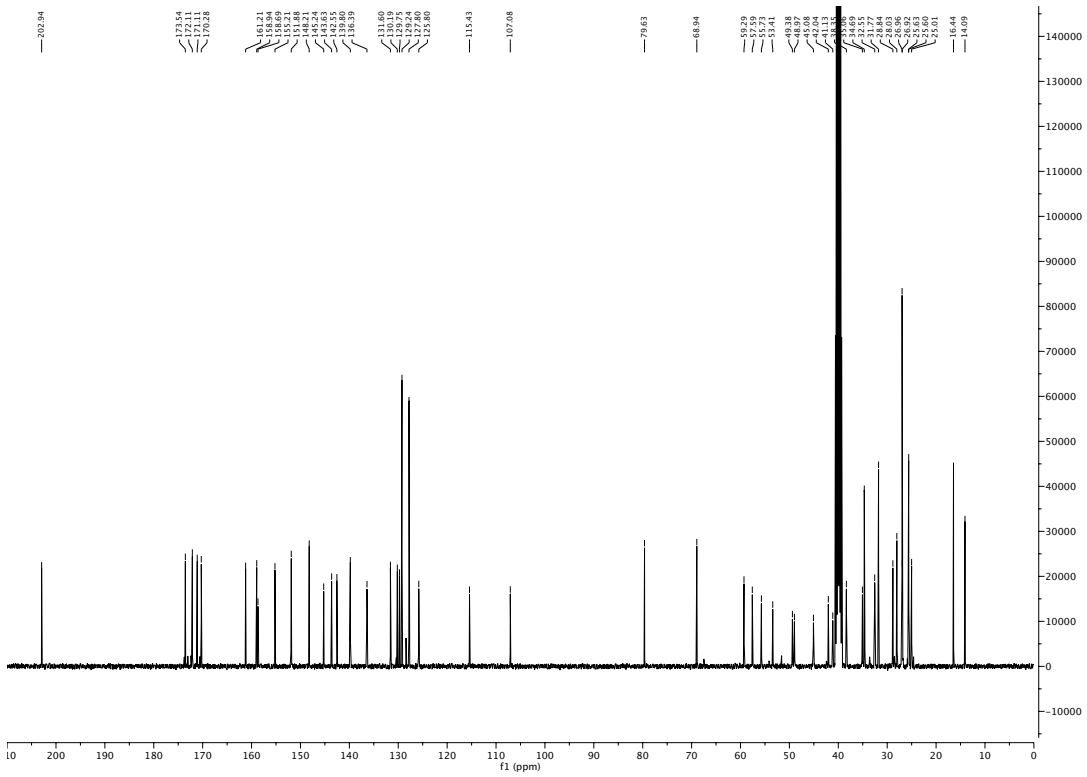
¹³C NMR spectrum of MS28.



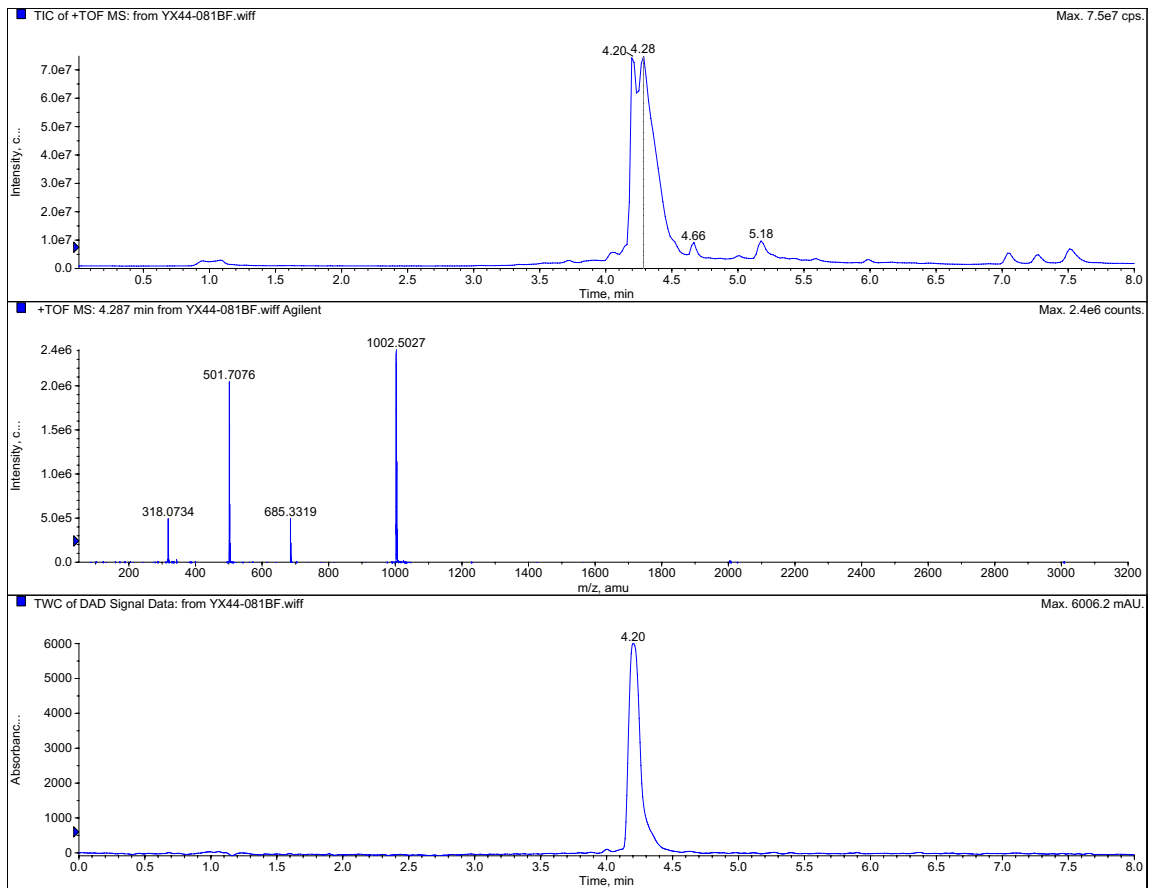
LC-MS spectrum of MS28.



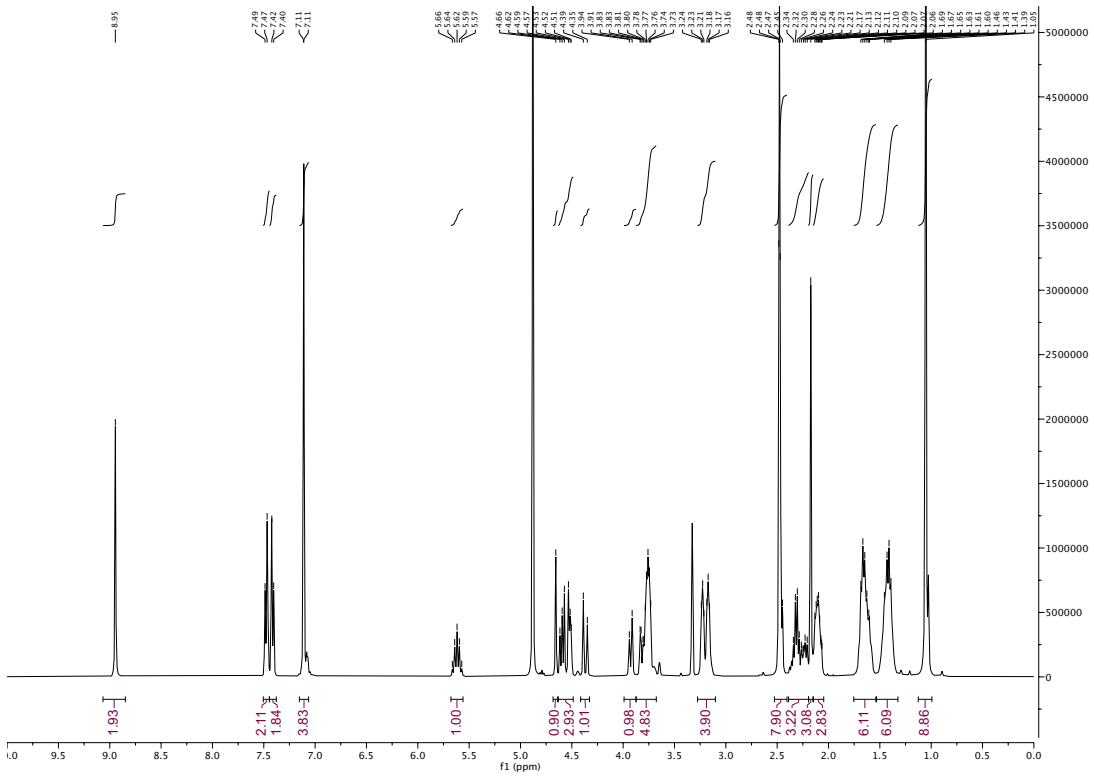
¹H NMR spectrum of MS28N1.



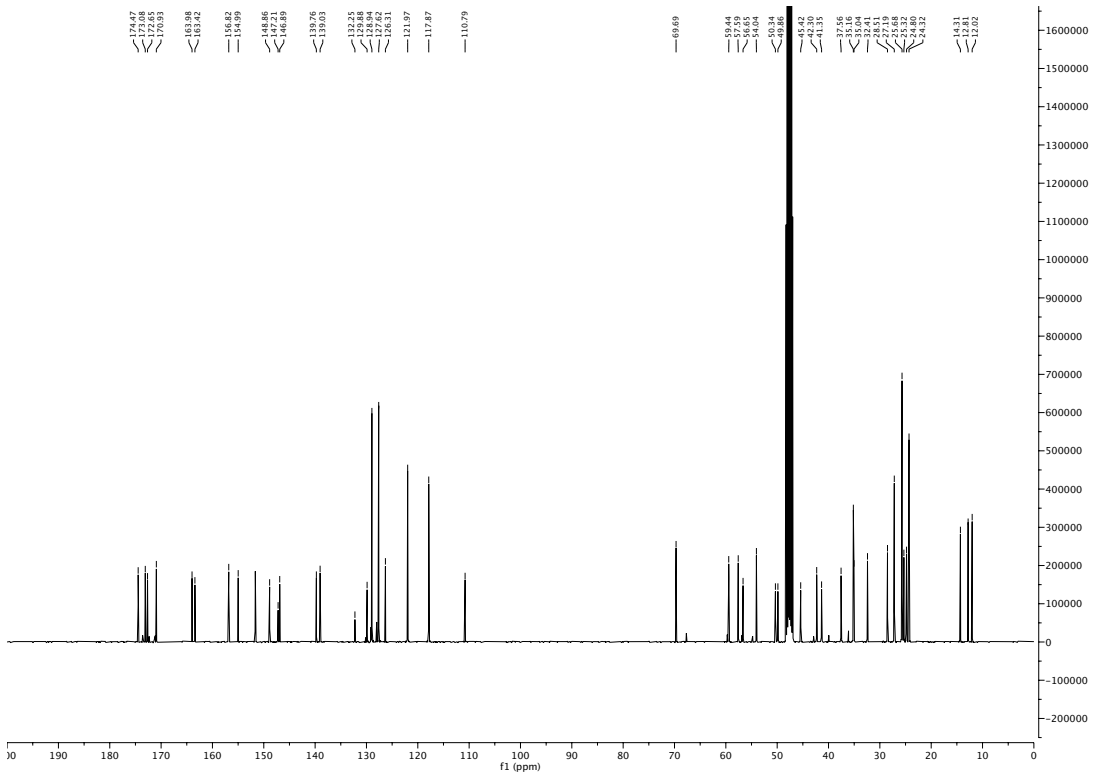
^{13}C NMR spectrum of MS28N1.



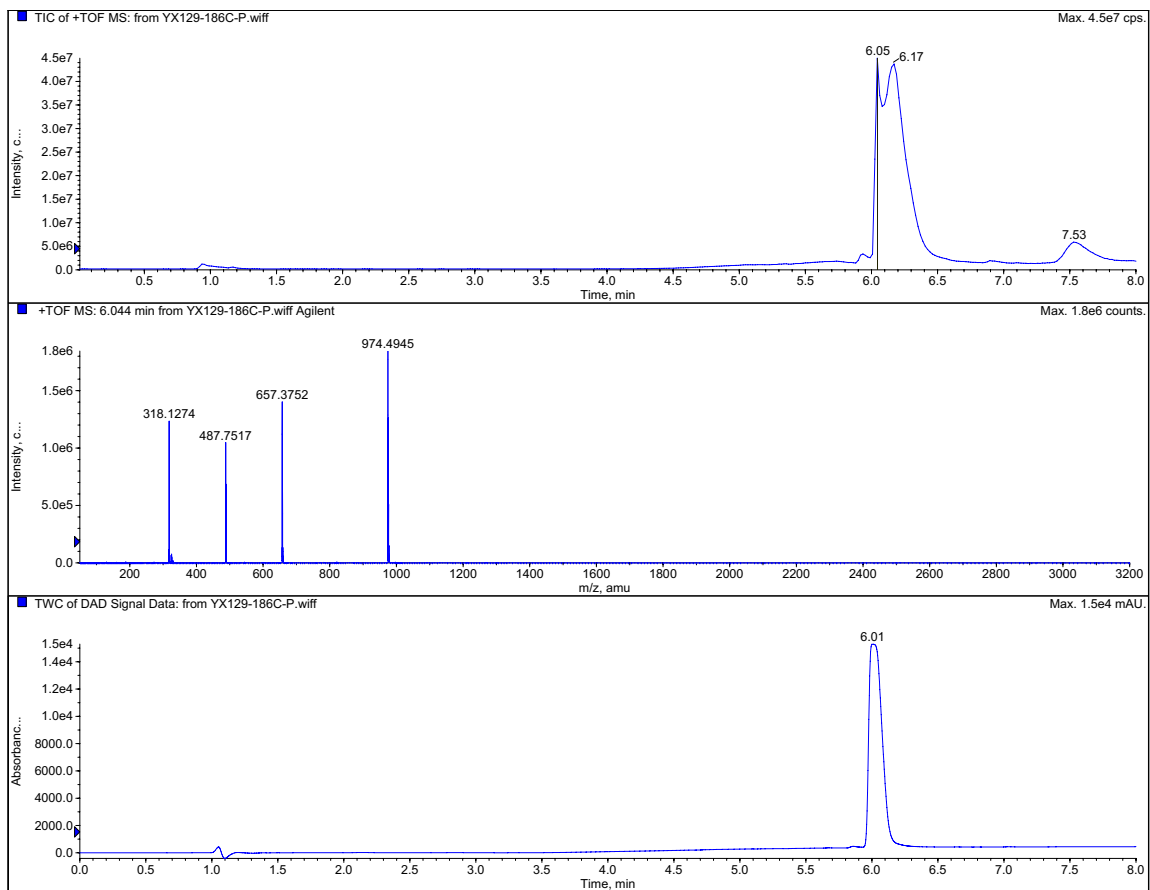
LC-MS spectrum of MS28N1.



¹H NMR spectrum of MS28N2.



¹³C NMR spectrum of MS28N2.



LC-MS spectrum of MS28N2.